# FINITE ELEMENT BASED EXPRESSIONS FOR LORENTZ, RELUCTANCE AND MAGNETOSTRICTION FORCES

Koen Delaere, *Ward Heylen, Ronnie Belmans, Kay Hameyer

*Dept. Electrical Eng. ESAT-ELEN, Katholieke Universiteit Leuven, Kardinaal Mercierlaan 94, B3001 Heverlee, Belgium.*
**Dept. Mechanical Eng. PMA, Katholieke Universiteit Leuven, Celestijnenlaan 200C, B3001 Heverlee, Belgium.*

**ABSTRACT** – The magnetic and mechanical finite element systems are combined into one magnetomechanical system. Investigating the coupling terms results in a finite element expression for the magnetic forces (Lorentz force and reluctance force) for both the linear and nonlinear case. The material deformation caused by magnetostriction is represented by an equivalent set of mechanical forces, giving the same strain to the material as magnetostriction does. The resulting magnetostriction force distribution is superposed onto other force distributions (external mechanical forces, magnetic forces) before starting the mechanical deformation or vibration analysis. This procedure is incorporated into a weakly-coupled cascade solving of the magnetomechanical problem.

**KEYWORKDS** – magnetic forces, magnetostriction, coupled problems, finite element analysis

## 1. INTRODUCTION

The main source of acoustic noise radiated by electric machines are the radial stator vibrations. Although this deformation is mainly caused by radial reluctance forces on the stator teeth (Maxwell stresses on the air-iron interface), magnetostriction effects can also contribute significantly to the deformation [1]. In order to be able to compute stator deformations, a *local* force expression is required. Here, based upon the coupled magnetomechanical finite element model, a nodal force expression is derived which covers both Lorentz forces and Maxwell stresses on the air-iron interface. The magnetostriction effect is represented by a set of nodal forces giving rise to the same deformation as magnetostriction does. The $\lambda(B)$ magnetostriction characteristic of the material (magnetostrictive strain $\lambda$ as a function of flux density $B$) is assumed to be known. The magnetostriction forces are determined for both isotropic and anisotropic materials, and for both plane stress and plane strain analysis.

## 2. THE COUPLED MAGNETO-MECHANICAL SYSTEM

Both magnetostatic and elasticity finite element methods are based upon the minimization of an energy function. The total energy $E$ of the electromechanical system consists of the *elastic energy U* stored in a body with (small elastic) deformation $a$ [2] and the *magnetic energy W* stored in a linear magnetic system with vector potential $A$ [3]:

$$E = U + W = \frac{1}{2} a^T K a + \frac{1}{2} A^T M A, \tag{1}$$

where $K$ is the mechanical stiffness matrix and $M$ is the magnetic 'stiffness' matrix. Considering the similar form of these energy terms, the following system of equations represents the numerically-coupled magnetomechanical system:

$$\begin{bmatrix} M & D \\ C & K \end{bmatrix} \begin{bmatrix} A \\ a \end{bmatrix} = \begin{bmatrix} T \\ R \end{bmatrix}, \tag{2}$$

where $T$ is the magnetic source term vector and $R$ represents external forces other than those of electromagnetic origin. Setting the partial derivatives of the total energy $E$ with respect to the unknowns $[A \ \ a]^T$ to zero, the combined system (2) with $T$=0, $R$=0 is retrieved:

$$\frac{\partial E}{\partial A} = M A + \frac{1}{2} a^T \frac{\partial K(A)}{\partial A} a = 0, \tag{3}$$

$$\frac{\partial E}{\partial a} = K a + \frac{1}{2} A^T \frac{\partial M(a)}{\partial a} A = 0, \tag{4}$$

giving the coupling terms $C$ and $D$. The coupling term $D$ can be used to represent magnetostriction effects in a numerically *strong* coupled analysis [4], but will not be considered here, so that $D$=0 and $T$=$MA$ (magnetostriction will be introduced further on in a numerically *weak* coupling approach). Rearranging the mechanical equation (4) into

$$Ka = -\frac{1}{2} A^T \frac{\partial M(a)}{\partial a} A = -CA = F_{mag}\,, \tag{5}$$

reveals a means to calculate the forces $F_{mag}$ internal to the magnetomechanical system. These magnetic forces are computed from vector potential $A$ and the *partial derivative* of the magnetic stiffness matrix $M$ with respect to deformation $a$. This procedure to obtain the magnetic forces $F_{mag}$ is equivalent to applying the virtual work principle to the magnetic energy $W$ for a virtual displacement $a$:

$$F_{mag} = -\frac{\partial W}{\partial a} = -\frac{\partial}{\partial a}\left[\frac{1}{2} A^T M(a) A\right], \tag{6}$$

where vector potential $A$ has to remain unchanged (constant flux). For the non-linear case, the matrix $M$ is a function of the magnetic field and displacement: $M(A,a)$. The magnetic energy $W$ is now given by the integral

$$W = \int_0^A T^{\mathrm{T}}\, dA = \int_0^A A^T M\, dA\,, \tag{7}$$

where $T$=$MA$ and $M^{\mathrm{T}}$=$M$ was used. The force expression (6) now becomes

$$F_{mag} = -\frac{\partial W}{\partial a} = -\int_0^A A^{\mathrm{T}} \frac{\partial M(A,a)}{\partial a} dA\,. \tag{8}$$

Note that adding a constant to $A$ indeed does not change the value of the integrals in (7) and (8). For $D$=0, the initial coupled system (2) can therefor be rearranged into the decoupled system

$$\begin{bmatrix} M & 0 \\ 0 & K \end{bmatrix} \begin{bmatrix} A \\ a \end{bmatrix} = \begin{bmatrix} T \\ R + F_{mag} \end{bmatrix}, \tag{9}$$

and solved in a cascade approach.

## 3. THE PARTIAL DERIVATIVE ∂M/∂a

The derivation $\partial M/\partial a$ is illustrated for the nonlinear case, using first order 2D triangular elements for simplicity. For the magnetic element matrix [5]

$$M_{ij}^e = \frac{\nu}{4\Delta}[b_i b_j + c_i c_j]\,, \tag{10}$$

with reluctivity $\nu$, element area $\Delta$ and the well-known shape function coefficients $a_1=x_2y_3-x_3y_2$, $b_1=y_2-y_3$, $c_1=x_3-x_2$. The partial derivative of (10) with respect to $u_1$ ($a_i=[u_i\, v_i]^{\mathrm{T}}$) is

$$\frac{\partial M_{ij}^e}{\partial u_1} = \frac{\nu}{4\Delta}\begin{bmatrix} 0 & c_1 & -c_1 \\ c_1 & 2c_2 & c_3 - c_2 \\ -c_1 & c_3 - c_2 & -2c_3 \end{bmatrix} - \frac{b_1}{2\Delta} M_{ij}^e + \frac{\partial \nu}{\partial u_1}\frac{M_{ij}^e}{\nu}\,. \tag{11}$$

Similar expressions are found for the partial derivative of $M^e$ with respect to alternative displacements ($u_2$, $u_3$, $v_1$, $v_2$ and $v_3$). The third term in (11) requires some attention. The reluctivity $\nu$ depends on flux density $B$ according to the saturation characteristic of the material. In the finite element code used here, the material characteristic is stored in $\nu(B^2)$ format [3][5]. For first order triangles, $B^2$ is given by

$$B^2 = B_x^2 + B_y^2 = \frac{1}{4\Delta^2}(c_1A_1 + c_2A_2 + c_3A_3)^2 + \frac{1}{4\Delta^2}(b_1A_1 + b_2A_2 + b_3A_3)^2 , \tag{12}$$

where $b_i$ and $c_i$ are the common shape function coefficients and $A_i$ is the vector potential on node $i$. Since in (12) only $c_2$ , $c_3$ and $\Delta$ depend on $u_1$ , the third term in (11) can be calculated explicitly:

$$\frac{\partial \nu}{\partial u_1} = \frac{d\nu(B^2)}{dB^2}\frac{\partial B^2}{\partial u_1} \tag{13a}$$

$$= \frac{d\nu(B^2)}{dB^2}\frac{1}{\Delta}\left[B_x(A_2 - A_3) - b_1B^2\right] \tag{13b}$$

$$= \frac{d\nu(B^2)}{dB^2}\, G_{u1}\, B^2 . \tag{13c}$$

In (13c), all factors independent of $B^2$ are gathered in $G_{u1}$. The actual value of $d\nu/dB^2$ is retrieved from the material characteristic. The factor $d\nu/dB^2$ acquires significant values only in elements that are heavily saturated; in these elements the third term in (11) becomes an important force component and must not be neglected.
In the non-linear expression (8), the integral values of the three terms in (11) are required. The integrals are calculated per element ($A_0$=[$A_{1,0}$ $A_{2,0}$ $A_{3,0}$]$^{\mathrm{T}}$) using $A$=$tA_0$, so that $dA$=$A_0dt$, $B^2$= $B_0^2$ $t^2$ and $d(B^2)$=2 $B_0^2$ $tdt$. For the first two terms in (11), the integral counterpart is found by replacing $\nu$ by the following integral:

$$\nu \rightarrow \frac{1}{2B_0^2}\int_0^{B_0^2} \nu(B^2)\, d(B^2) , \tag{14}$$

where $B_0$ is the actual value of the flux density in the element under consideration. The integral of the third term in (11) reduces to

$$\int_0^{A_0} A^{\mathrm{T}} \frac{\partial \nu}{\partial u_1}\frac{M_{ij}^e}{\nu} dA = \frac{1}{\nu}A_0^{\mathrm{T}} M_{ij}^e A_0 \left( \int_0^1 \frac{\partial \nu}{\partial u_1} t\, dt \right) , \tag{15}$$

since $M_{ij}^e / \nu$ is short for $[b_ib_j+c_ic_j]/4\Delta$ and does not depend on $\nu$ or $A$. Using (13c), the integral in (15) becomes

$$\int_0^1 \frac{\partial \nu}{\partial u_1} t\, dt = G_{u1} \int_0^1 \frac{d\nu}{dB^2} B^2\, t\, dt \tag{16}$$

$$= \frac{G_{u1}}{2B_0^2} \int_0^{B_0^2} \frac{d\nu}{dB^2} B^2\, d(B^2) \tag{17}$$

$$= \frac{G_{u1}}{2B_0^2} \int_{\nu^*}^{\nu_0} B^2 d\nu , \tag{18}$$

where $\nu$* is the reluctivity in the linear part of the material characteristic. From the integral in (18) it is seen that the third term in (11) is linked to the co-energy in the system, while the first two terms of (11) are linked to the energy integral in (14). The relation between both energies is given by

$$\int_{\nu^*}^{\nu_0} B^2\, d\nu = B_0^2 \nu_0 - \int_0^{B_0^2} \nu(B^2) d(B^2) , \tag{19}$$

so that only one integral needs to be evaluated. Similar expressions are found for the partial derivatives with respect to the other displacements ($u_2$, $u_3$, $v_1$, $v_2$ and $v_3$).

## 4. RELUCTANCE AND LORENTZ FORCES

Expression (8) for the force $F_{mag}$ was derived in a general fashion, not focussing particularly on permeability interfaces or regions with imposed current. Any permeability interfaces will contribute greatly to the $\partial M/\partial a$ summation over a node that lies on the interface and will yield the same local force value as applying Maxwell stress on the interface does. Elements with current density will affect the vector potential profile in such a way that, when (8) is used, exactly the Lorentz force acting on that element is obtained. Expression (5) (the linear version of expression (8)) is therefor equivalent to the well-known force expression [6]

$$F = J \times B - \frac{1}{2} H^2 \nabla\mu \,, \qquad (20)$$

where the second term can also be written as [7]

$$-\frac{1}{2} H^2 \nabla\mu = \left[ \frac{b_n^2}{2}\left( \frac{1}{\mu_0} - \frac{1}{\mu} \right) - \frac{h_t^2}{2}(\mu_0 - \mu) \right] \mathbf{n} \,, \qquad (21)$$

where $b_n$ is the normal component of flux density and $h_t$ is the tangential component of magnetic field at the interface between materials with permeability $\mu_0$ and $\mu$. ($\mathbf{n}$ is the unit normal vector). Expression (8) is equivalent to (20) since they can both be derived using the virtual work principle.

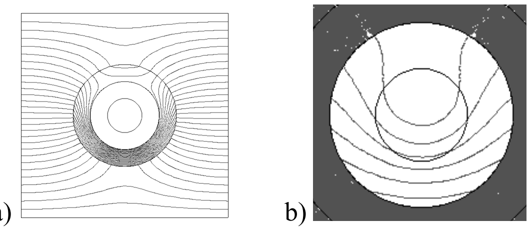

a) b)

Fig.1 a) Conductor shielded from external field by permeable ring, b) Magnetic field around conductor.

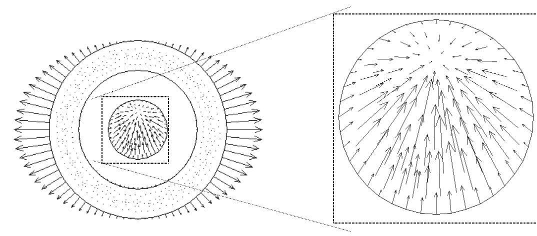

Fig.2 Force distribution for shielding problem obtained using (8), *inset*: detail of force distribution on conductor.

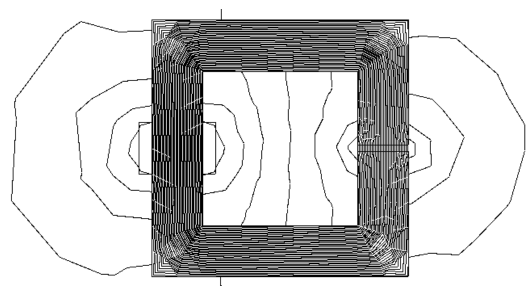

Fig.3 Magnetic field in iron C-core (excited by coil on left leg, airgap in right leg).

Fig.1a shows a conductor with current $I$ in a uniform external magnetic field $B_e$, but shielded by a ring of magnetic material. The Lorentz force per meter on the conductor without shielding is $F_{tot} = I\,B_e$. With shielding the Lorentz force is $F_s = I\,B_s$ where $B_s$ is the (much smaller) homogeneous field at the conductor after shielding. Fig.1b shows the magnetic field using a very large number of flux lines so that the small field at the conductor becomes visible. The field shown in Fig.1b is the sum of the homogeneous field $B_s$ and the field of the conductor current itself. Fig.2 shows the result of force expression (8) with a more detailed view of the forces on the conductor (inset). The sum of the nodal forces on the conductor gives exactly $F_s = I\,B_s$. The sum of the nodal forces on the shielding ring gives $F_M = F_{tot} - F_s = I\,B_e - I\,B_s$ so that the total force on the ring-conductor system again gives $F_{tot}$ [8, p.368].

Fig.3 shows the equipotential lines of the flux in a C-core with an airgap in the right leg and excited by a coil on the left leg with $10^4$ Ampèreturns (in order to obtain heavy saturation). Fig.4 shows the corresponding force pattern obtained when applying the force expression (8) to the magnetic field in the C-core. The forces on the airgap edges represent the reluctance

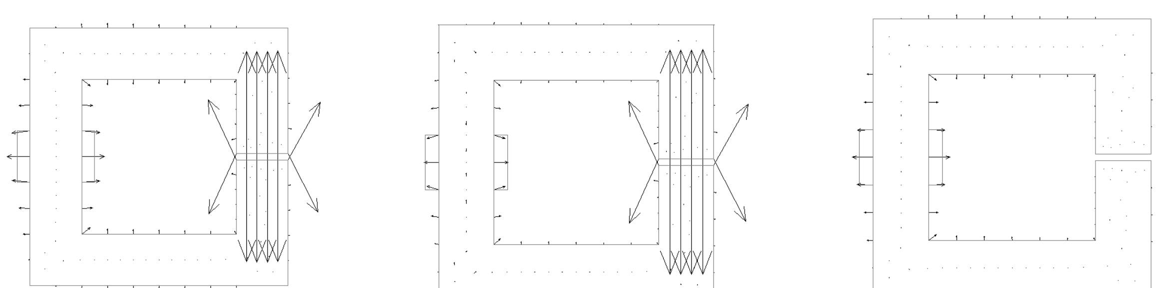

a) b) c)

Fig.4 Magnetic forces on iron C-core (small horizontal airgap in the right leg) found using (8) and (11): a) total force pattern, b) linear part of force pattern ($\mu$ considered constant), c) nonlinear part of force pattern.

forces. Fig.4a shows the total force pattern, while Fig.4b shows the force pattern obtained using only the first two terms in (11). This is equivalent to keeping the permeability of the material constant (for linear materials, expression (5) can be used). In Fig.4a and 4b, the forces on the airgap edges are due to the $b_n$ term in (21), while the forces on the sides of the C-core are due to the $h_t$ term in (21). Fig.4c shows the contribution of the third term in (11) to the force pattern (magnified by a factor 2). It can be seen that the saturated areas (left leg is more saturated than upper and lower leg) want to increase their cross-section.

## 5. MAGNETOSTRICTION FORCES

Effects where there is a mutual influence between the mechanical deformation or stress and the magnetisation $\mu_0 M$ in the material, are called *magnetomechanical effects*. The most important is the *magnetostriction effect* $\lambda(B)$, pertaining to the strain $\lambda$ of a piece of material due to its magnetisation. The *inverse magnetostriction* effect is the dependency of the magnetisation $\mu_0 M$ on the stresses $\sigma$ occurring in the material. Since stress influences magnetisation, it will also influence the magnetostriction itself and turn the $\lambda(B)$ characteristic into a $\lambda(B,\sigma)$ dependency [9]. Usually there is no relevant volume change due to magnetostriction [10].

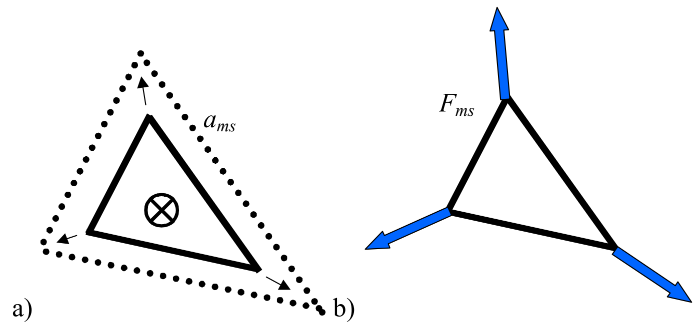


Fig.5 The center of gravity of the element is considered to be fixed while the magnetostrictive expansion $\lambda(B^e)$ is applied to the nodes. This deformation is represented by a set of mechanical forces $F_{ms}$.

Magnetostriction is implemented in the coupled system by a force distribution $F_{ms}$ that is added to $R$ and $F_{mag}$ in (9). By *magnetostriction forces* we indicate the set of forces that induces the same strain in the material as magnetostriction does. This approach is similar to how thermal stresses are usually taken into account [11]. To evaluate thermal stresses, the thermal expansion of the free body (no boundary conditions) is calculated based upon the temperature distribution, and then the thermal stresses are found by deforming the expanded body back into its original shape (back inside the original boundary conditions). To calculate magnetostriction forces, the expansion of the free body due to magnetostriction is found based upon the magnetic flux density, and the magnetostriction forces are found as the reaction to the forces needed to deform the expanded body back into the original boundary conditions.

For finite element models, this can be performed on an element by element basis, where the midpoint of the element (the centre of gravity) can be used as a locally fixed point. The magnetostrictive deformation of the element, i.e. the displacement of the three nodes with respect to the midpoint, is found using the element's flux density $B^e$ and the $\lambda(B)$ characteristic of the material. Fig.5a shows the original element (solid line) and the deformed element (dashed line) after applying the magnetostrictive strain $\lambda(B^e)$ keeping the centre fixed. The magnetostriction forces $F_{ms}$ (Fig.5b) are the set of forces inducing the same deformation.

*3.2 Strain for isotropic materials*

Fig.6 shows a typical magnetostriction characteristic for isotropic 3% SiFe (solid lines) as a function of tensile stress. For isotropic materials, the local *xy*-axes of the element are chosen so that the *x*-axis coincides with the flux density vector **B**. Usually magneto-striction will leave the volume unchanged [10], so that the strains in the local frame are given by

$$\begin{aligned} \lambda_x &= \lambda \\ \lambda_y &= \lambda_t = -\lambda/2 \\ \lambda_z &= \lambda_t = -\lambda/2 \end{aligned} \tag{22}$$

where $\lambda=\lambda(B)$ is the magnetostrictive strain in the direction of **B**

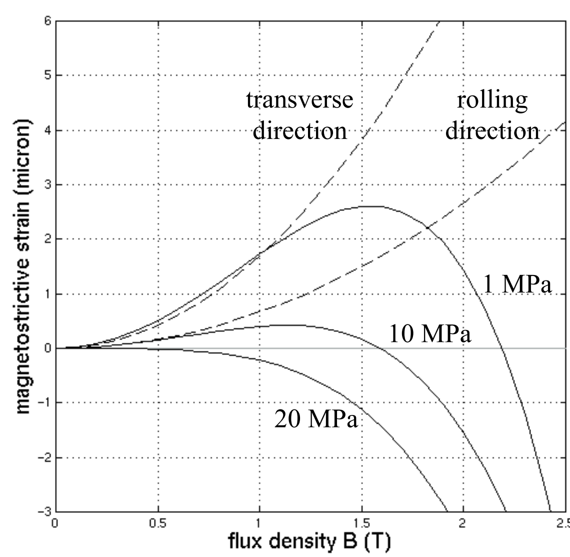


Fig.6 Magnetostrictive material characteristics of non-oriented 3% SiFe (solid lines, as a function of tensile stress) and M330-50A (dashed lines, for rolling and transverse direction).

and $\lambda_t$ is the magnetostrictive strain in the transverse directions. In a 2D *plane strain* analysis, the thickness ($z$-direction) of the material has to remain constant and an additional $z$-stress needs to be applied in order to obtain $\lambda_z$=0. This adjusts the strains in (22) to

$$\begin{aligned} \lambda_x &= \lambda + \nu\lambda_t \\ \lambda_y &= \lambda_t + \nu\lambda_t \\ \lambda_z &= \lambda_t - \lambda_t = 0 \end{aligned} \tag{23}$$

where ν is the Poisson modulus of the material.

*3.3 Strain for anisotropic materials*

Fig.6 shows a typical magnetostriction characteristic for anisotropic M330-50A steel (dashed lines). As an approximation of the anisotropic behavior, the flux density vector is decomposed into a $B_x$ and a $B_y$ component in the element's local $xy$-axis, arranged so that the $x$-axis coincides with the rolling direction, and the $y$-axis with the perpendicular direction. The rolling direction curve $\lambda_{\mathrm{RD}}(B)$ is then used with $B_x$ as input, and the perpendicular direction curve $\lambda_{\mathrm{PD}}(B)$ with $B_y$ as input, giving

$$\begin{aligned} \lambda_x &= \lambda_{\mathrm{RD}}(B_x) - \nu\lambda_{\mathrm{PD}}(B_y) \\ \lambda_y &= \lambda_{\mathrm{PD}}(B_y) - \nu\lambda_{\mathrm{RD}}(B_x) \\ \lambda_z &= -\lambda_{\mathrm{RD}}(B_x) - \nu\lambda_{\mathrm{PD}}(B_y) \end{aligned} \tag{24}$$

Depending on the actual anisotropic behavior of the material, a more accurate strain description can be used, e.g. taking magnetostrictive shear $\lambda_{xy}$ into account [12]. A similar correction as in (23) can be made for the plane strain case.

*3.4 Displacement and force*

Still working in the local $xy$-axes, the element's strains $\lambda^e_x$ and $\lambda^e_y$ are converted into three nodal displacements $a^e_{ms,i}=(a^e_{x,i}, a^e_{y,i})$, $i$=1,2,3 considering the midpoint of the element $(x^e_m, y^e_m)$ as fixed:

$$\begin{bmatrix} a_{x,i} \\ a_{y,i} \end{bmatrix} = \begin{bmatrix} x_i - x_m^e \\ y_i - y_m^e \end{bmatrix} \begin{bmatrix} \lambda^e \\ \lambda_t^e \end{bmatrix}, \; i=1,2,3 \; , \tag{25}$$

with $(x_i, y_i)$ the co-ordinate of node $i$. The mechanical stiffness matrix allows us to convert the displacements $a^e_{ms}$ into a set of forces using

$$F_{ms}^e = K^e a_{ms}^e \; . \tag{26}$$

This procedure is performed element by element; it cannot be done for the whole mesh at once, because the displacements $a^e_{ms}$ due to the different elements surrounding a node, cannot be summed. The resulting nodal forces $F^e_{ms}$ however, *can* be summed. As a result, the distribution of magnetostriction forces $F_{ms}$ is obtained and added to the other force distributions:

$$\begin{bmatrix} M & 0 \\ 0 & K \end{bmatrix} \begin{bmatrix} A \\ a \end{bmatrix} = \begin{bmatrix} T \\ R + F_{mag} + F_{ms} \end{bmatrix} . \tag{27}$$

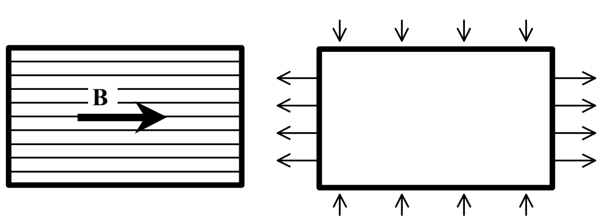


Fig.7. The set of forces (right) representing the strain caused by magnetostriction due to the magnetic field **B** (left), consists of a set forces parallel to **B** and a set forces perpendicular to **B**.

The magnetostriction forces can now be added to any other set of forces to give the total force distribution acting on the device, which can be readily used for deformation or vibration calculation [13].

Note that due to the fact that magnetostriction usually leaves the volume unchanged, the magnetostrictive 'Poisson modulus' is $\nu_{ms}$=0.5, while the mechanical Poisson modulus of the material is about ν=0.3. This means that, next to a set of forces *parallel* to **B**, there will always be a set of forces *perpendicular* to **B** (Fig.7).

## 6. EXAMPLE: 6-POLE SYNCHRONOUS MACHINE STATOR

Fig.8 shows the magnetic field in one pole of a six-pole synchronous machine. $B_{max}$ in the teeth is 1.26 T corresponding to $\lambda = 2.3$ μm/m for 3% SiFe with 1 MPa tensile stress. Fig.9 shows the magnetostriction forces on the stator for the magnetic field of Fig.8: Fig.9a for a stator of isotropic non-oriented 3% SiFe and Fig.9b for a stator of anisotropic M330-50A (both materials were modeled with Young modulus $E = 2.2\ 10^{11}$ Pa and $\nu = 0.3$). In the areas of high flux density in the stator, there are magnetostriction forces parallel to the flux lines and also a set of magnetostriction forces perpendicular to the flux lines, both seeking to *increase* the circumference of the stator. In the anisotropic case, the general magnetostriction force pattern remains the same, but the forces appear slanted. Fig.10 repeats Fig.9a but also shows the reluctance forces $F_{mag}$ for the magnetic field of Fig.8. It can be seen that $F_{ms}$ and $F_{mag}$ are of the same order of magnitude (the size of the nodal force vectors on the teeth tips is 25 N).

## 7. CONCLUSION

The mechanical and magnetic finite element system are combined into one magnetomechanical system. This results in a finite element based expression for nodal forces representing both Lorentz forces and reluctance forces (Maxwell stresses on material interfaces), for both linear and nonlinear materials. The magnetostriction of the material is taken into account by a force distribution (magnetostriction forces) that induces the same strain into the material as magnetostriction does. This is done for both isotropic and anisotropic materials. These force distributions can be added to other force distributions to start a subsequent mechanical deformation or vibration analysis.

## ACKNOWLEDGEMENTS

The authors are grateful to the Belgian "Fonds voor Wetenschappelijk Onderzoek Vlaanderen (FWOV)" for its financial support; Koen Delaere has a FWOV scholarship. The authors thank the Vlaamse Wetenschappelijke Stichting for its financial support and the Belgian Ministry of Scientific Research for granting the IUAP No.P4/20 on Coupled Problems in Electromagnetic Systems. The Research Council of the K.U.Leuven supports the basic numerical research.

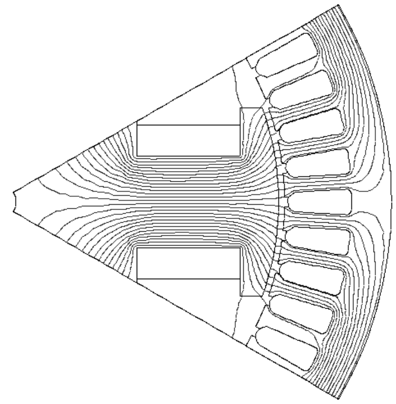

Fig.8 Magnetic field in one pole of a six-pole synchronous machine.

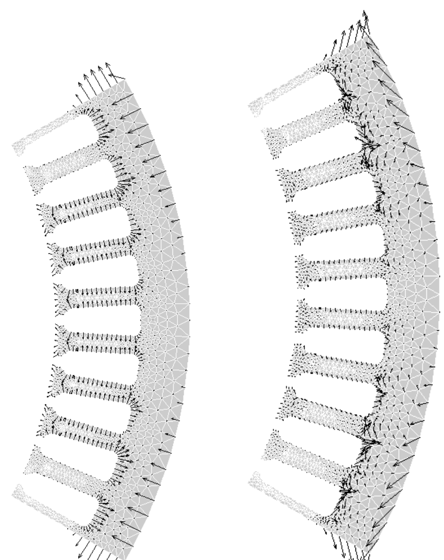

a) b)

Fig.9 Magnetostriction forces on stator for
a) isotropic non-oriented 3% SiFe,
b) anisotropic M330-50A.

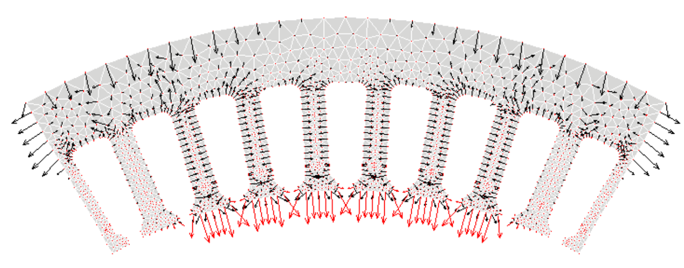

Fig.10 Comparison between reluctance forces (on the teeth tips) and magnetostriction forces (on the stator surface).

## REFERENCES


[1] Låftman L. (1995), The Contribution to Noise from Magnetostriction and PWM Inverter in an Induction Machine, Ph.D. thesis, Department of Industrial Electrical Engineering and Automation, Lund Institute of Technology, KF Sigma, Sweden.

[2] Zienkiewicz, O.C., Taylor, R.L. (1989), The Finite Element Method, McGraw-Hill.

[3] Silvester, P.P., Ferrari R.L. (1996), Finite Elements for Electrical Engineers, Third Edition, Cambridge University Press.

[4] Delaere, K., Hameyer, K., Belmans, R. (2000), "Introducing magnetostriction into magnetomechanical analysis," Intern. Conf. on Electric Machines ICEM 2000, Espoo, Finland, 28-30 August, submitted for publication.

[5] Binns, K.J., Lawrenson, P.J., Trowbridge, C.W. (1992), The Analytical and Numerical Solution of Electric and Magnetic Fields, John Wiley & Sons.

[6] Woodson, H.H., Melcher, J.R. (1968), Electromechanical Dynamics, Part II: Fields, Forces and Motion, John Wiley & Sons, New York.

[7] Ren, Z. (1994), "Comparison of different force calculation methods in 3D finite element modelling," IEEE Transactions on Magnetics, Vol 30, no.5, September.

[8] Zahn, M. (1979), Electromagnetic Field Theory: a problem solving approach, John Wiley & Sons, New York.

[9] Jiles, D. (1991), Introduction to Magnetism and Magnetic Materials, Chapman & Hall.

[10] Cullity, B.D. (1972), Introduction to Magnetic Materials, Addison-Wesley (Series in Metallurgy and Materials), Philippines.

[11] Hirsinger, L. (1994), Etude des deformations magneto-elastiques dans les materiaux ferromagnetiques doux. Application a l'etude des deformations d'une structure de machine electriques, Ph.D. thesis, Laboratoire de Mecanique et Technologie, Universite Paris 6, (ISBN 2-11-088808-3).

[12] Pfützner, H., Hasenzagl, A. (1996), "Fundamental aspects of rotational magnetostriction," in Nonlinear Electromagnetic Systems, eds. A.J. Moses, A. Basak, pp.374-379, IOS Press, Cardiff.

[13] Delaere, K., Iadevaia, M., Sas, P., Belmans, R., Hameyer, K. (1999), "Coupling of numerical magnetic and experimental vibration analysis for electrical machines", 3rd Chinese International Conference on Electrical Machines CICEM99, Xi'an, P.R.China, 29-31 August, vol 1, pp.475-478.